

VIP Very Important Paper

Special
Collection

Optimization Strategies for the Anodic Phenol-Arene Cross-Coupling Reaction

Maximilian Hielscher, Elisabeth K. Oehl, Barbara Gleede, Julian Buchholz, and Siegfried R. Waldvogel*^[a]*Dedicated to Prof. Wolfgang Schuhmann on the occasion of his 65th birthday.*

Dehydrogenative phenol-arene cross-coupling by direct anodic oxidation is a promising alternative to reductive cross-coupling, especially for construction of smaller molecules. The reaction pathway via phenoxyl radicals allows for unusual regioselectivity. Nevertheless, the numerous electrolysis parameters pose a challenge for optimization, as they determine the yield and selectivity of the reaction. Using design of experiments, we present optimization strategies for two example reactions to

improve the space-time yield. In particular, coupling reactions with 2,6-dimethoxyphenol (syringol) were found to be very robust in the electrolysis at high current densities of up to 150 mA/cm². Cyclic voltammetry was used to classify combinations of phenols and arenes, on the basis of which the various clusters were optimized. Based on this classification, various biaryls were synthesized and isolated in yields of up to 85%.


Introduction


Non-symmetric biaryl moieties represent a frequently occurring structural motif and can be found in a variety of natural products,^[1] as building blocks of ligands for homogeneous catalysis^[2] and in material science.^[3] The formation of carbon-carbon bonds is one of the most important fields in modern organic synthesis, at the scale of (cross)coupling of small molecules up to late-stage steps in convergent synthesis.^[4] In classic chemistry, the synthesis of non-symmetric biaryls can take place in different ways. Transition metal catalysis has been well established for this type of reaction. In this generally two-step process, leaving groups are first installed on the respective coupling partners and then the C–C bond is formed using transition metals such as Pd,^[5] with loss of the leaving groups. Known methods use arylboronic acids,^[6] arylstannanes,^[7] benzoic acid derivatives,^[8] arylzinc,^[9] or arylmagnesium reagents.^[10] This leads to a multi-step sequence with intense workload, large chemical consumption, and excessive waste amount. A more efficient approach is the C–H activation of one coupling partner by a catalytically active transition metal species. Nevertheless, a leaving group still must be introduced at the second coupling partner.^[11]


Dehydrogenative coupling is possible using an oxidative protocol, resulting in reduced synthesis effort and thus more environmentally friendly approach. The coupling partners can be coupled directly by a terminal oxidizer.^[12,13] However, the corresponding reduced form of the oxidizer must be removed after the reaction and, in the case of metal salts, trace contaminations can remain in the product, which is a significant drawback in the production of pharmaceuticals. Electro-organic synthesis is a highly attractive alternative to the classical synthesis routes that can avoid the disadvantages mentioned above.^[14]

The use of electric current replaces terminal oxidizers and therefore provides an inherent safety in the reaction control at the same time, a shutdown of the current suppresses possible runaway reactions. Reagent waste can be almost completely avoided, so this method can be referred to as green chemistry.^[15] If the selectivity is sufficient and workup not too tedious the organic electrosynthesis can pay off.^[16] For direct anodic cross-coupling to achieve preparative amounts of product, the use of a galvanic protocol in a two-electrode setup rather than a potential-controlled three-electrode setup is necessary.^[17,18] This poses challenges in terms of cross-coupling selectivity and product stability during conversion, as no redox filter is active in terms of potential control. However, for the conversion of the initial 95% of substrate no strong deviation of the required oxidation potential is required.^[18] For phenol-arene coupling, the use of boron-doped diamond (BDD) electrodes in combination with fluorinated alcohols such as 1,1,1,3,3,3-hexafluoropropan-2-ol (HFIP) has proven successful; this system has a potential window range larger than 5 V, while HFIP stabilizes reaction intermediates by solvation, which has a positive effect on yield and selectivity.^[19,20,21] The BDD electrodes can be considered as inert, metal-free and long-term stable materials.^[22] Furthermore, the electrolysis conditions as well as the substrate combinations with their respective oxidation potentials and their nucleophilicity play a decisive role.^[13]

[a] M. Hielscher, E. K. Oehl, Dr. B. Gleede, J. Buchholz, Prof. Dr. S. R. Waldvogel
Department of Chemistry
Johannes Gutenberg University
Duesbergweg 10–14, 55128 Mainz, Germany
E-mail: waldvogel@uni-mainz.de

 Supporting information for this article is available on the WWW under <https://doi.org/10.1002/celec.202101226>

 An invited contribution to the Wolfgang Schuhmann Festschrift.

 © 2021 The Authors. ChemElectroChem published by Wiley-VCH GmbH. This is an open access article under the terms of the Creative Commons Attribution Non-Commercial NoDerivs License, which permits use and distribution in any medium, provided the original work is properly cited, the use is non-commercial and no modifications or adaptations are made.

Rational optimization strategies are necessary to understand the relationship of the numerous reaction parameters and to control yield and selectivity, by suppressing the formation of minor components, as well as the over-oxidation of the desired product (Figure 1).^[23] Statistics-based methods such as Design of Experiments (DoE) have already proven extremely helpful for this purpose in the optimization of electrochemical conversions. In particular, the space-time yield of electrochemical reactors has been significantly improved.^[24] To obtain optimized conditions for different substrates, substrate properties must be included in the modelling, like predictive modelling approaches from complex-based homogeneous catalysis.^[25]

Under optimized conditions, direct anodic oxidative coupling is a useful method with good scalability on both laboratory and industrial scales. Only the coupling partners, supporting electrolyte and solvent are used for the reaction. All non-converted components can be recovered and reused after electrolysis. In the last decade, we have already demonstrated that the method has a broad application in the cross-coupling of phenols with arenes,^[26–28] other phenols,^[29,30] anilines,^[20,31] and heterocycles such as benzothiophenes.^[21,32]

Results and Discussion

Here we report on the electrochemical synthesis of new non-symmetric biaryls with a focus on upstream optimization of our previously published synthesis conditions. In the last decade, our established method has repeatedly shown that it can enable the synthesis of completely new substrate patterns, which were previously not accessible with classical chemistry. We started our investigation of further anodic phenol-arene coupling reactions by pre-screening at 1 mmol scale in 5 mL Teflon cells. BDD was used as electrode material, methyltributylammonium methyl sulfate (MTBS) as supporting electrolyte and HFIP as solvent. The electrolysis was performed in an undivided beaker-type cell under constant current conditions. Selectivity and reaction outcome were determined by GC and GCMS, respectively.

Typical minor byproducts are the corresponding homo-coupling products of phenols, oligomerization products from phenols and arenes, and over-oxidation products of the coupling products (Figure 2, right). However, benzylic oxidations and follow-up reactions may occur. With this approach, we were able to rapidly identify suitable substrate combinations for cross-coupling reactions to previously unknown products. The starting point of the screening experiments was the parameter space, in which our previously optimized conditions are found. Using the parameter set B, suitable substrate pairs

Challenges of the Dehydrogenative Anodic Phenol-Arene C-C Cross-Coupling Reaction

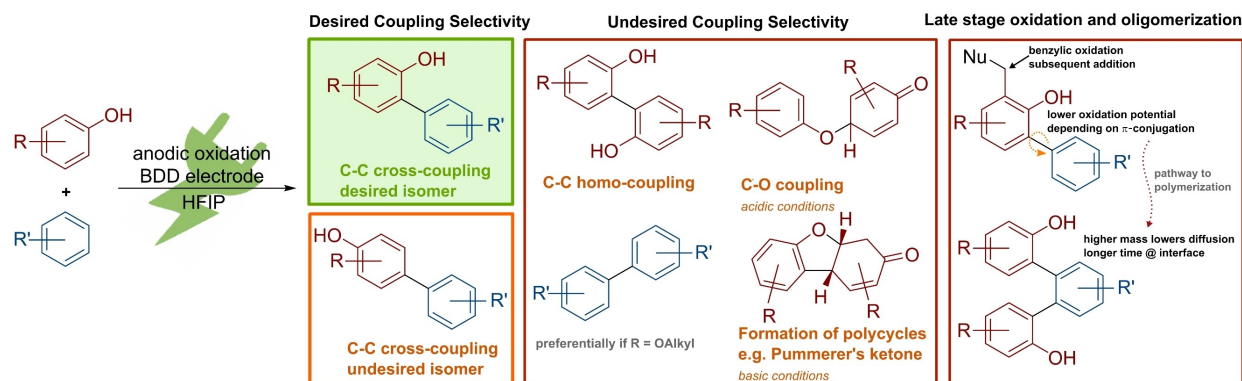


Figure 1. Typical challenges in dehydrogenative anodic phenol-arene cross-coupling with respect to the product range of this reaction.

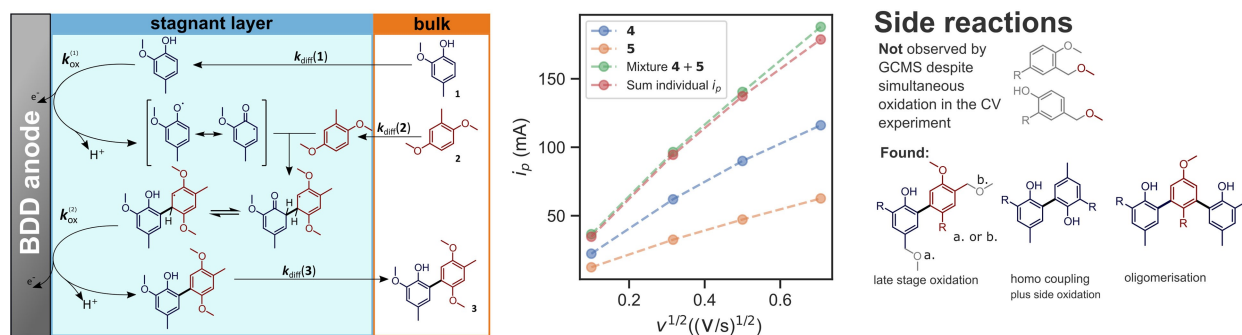


Figure 2. Mechanism of dehydrogenative anodic phenol-arene cross-coupling at BDD anodes (left). Randles-Sevcik plot of the single substrate 4 and 5, as well as the mixture of both (middle), side components found during the optimization (right).

were determined on a 5 mL scale. Promising substrate combinations were scaled-up by the factor of five using two sets of electrolysis conditions to test the reaction outcome. This includes ones with higher substrate loading and enhanced current density as well as lower loading and lower current density (A: $j = 10.2 \text{ mA/cm}^2$, $[\text{phenol}] = 0.20 \text{ M}$, $[\text{arene}] = 0.70 \text{ M}$, $[\text{MTBS}] = 80 \text{ mM}$, $Q = 2 F$ (per phenol), $V = 25 \text{ mL}$, $T = 10^\circ\text{C}$. B: $j = 5.2 \text{ mA/cm}^2$, $[\text{phenol}] = 0.15 \text{ M}$, $[\text{arene}] = 0.45 \text{ M}$, $[\text{MTBS}] = 90 \text{ mM}$, $Q = 2 F$ (per phenol), $V = 25 \text{ mL}$, $T = 50^\circ\text{C}$). In three cases, cross-coupling yields were quite similar despite condition set A or B applied. When we studied the oxidation behavior of the substrates by cyclic voltammetry, we found that these three combinations have only a small difference in half-wave potentials (0.1 V), whereas combinations outside this potential difference cause the yield of one set of conditions to significantly exceed over the others (Figure 3). While for 2,4-substituted phenols the conditions with higher phenol concentrations and current densities led to higher yields, using syringol (4) as a phenol component a lower concentration and current density showed about 20% higher yield. This was observed for both arenes with higher and lower oxidation potentials.

Following the postulated mechanism (Figure 2, left), the phenol being oxidized at the anode is rapidly deprotonated to form a neutral radical species. To promote the cross-coupling reaction, the arene component is added in excess to favor the nucleophilic attack on the phenoxy radical formed. It has also been shown that substrate combinations wherein the arene has the lower half-wave potential than the phenol allow for successful C–C cross-coupling (I and IV). In the case of 4 and 3,4-dimethoxytoluene (5) (III), oxidation potentials show only a small potential difference and, in a CV experiment the oxidative peak currents of the individual components sum up to the peak

current of the mixture, the cross-coupling reactions reveal a high selectivity. Side reactions such as benzylic oxidation of the substrates towards benzyl ethers could not be detected by GCMS. Fortunately, remaining starting material can be easily recovered and reused.

We started further optimization with a 2^{4-1} fractional factorial design with 4-methylguaiacol (1) and 2,5-dimethoxytoluene (2). Regarding the parameters and their limits, we have been guided by the anodic phenol arene cross-coupling studies carried out so far by our group (Table 1).^[26,27] The current density should be investigated in the elevated range of 10–20 mA/cm^2 to possibly achieve a higher space-time yield. The screening reactions were conducted in Teflon cells (electrolyte volume 5 mL) with an active anode area of 1.5 cm^2 in HFIP with 18 vol.% methanol as solvent mixture and MTBS as supporting electrolyte. Yields were determined by calibrated gas chromatography equipped with a FID detector. *n*-Octylbenzene served as an internal standard. The corner point experiments were carried out in duplicate and the central point experiments in triplicate. As a system response, the yield and selectivity were determined via GC-FID integrals with respect to the integral of the internal standard, as well as the initial amount of 1. The model was backward eliminated ($\alpha = 0.05$) and all non-significant terms were removed from the model (Figure 4). Similar to the already optimized case of phenol-phenol cross-coupling in

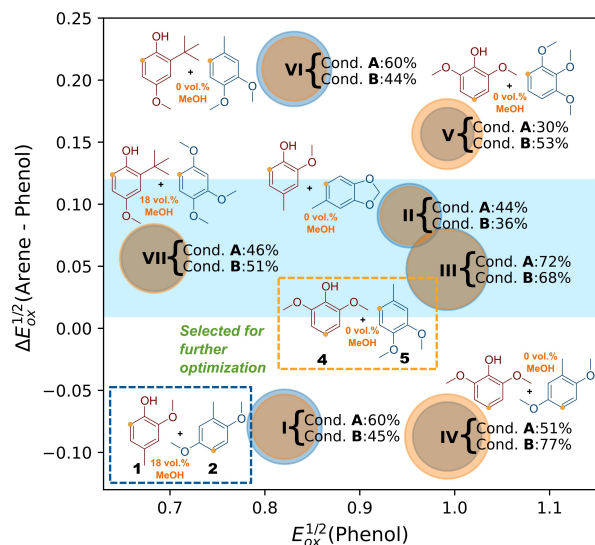


Figure 3. Comparison of isolated yields using two different sets of electrolysis conditions. The half-wave potential of the phenolic coupling partner (preferred coupling site indicated) and the difference of the half-wave potentials of phenolic and anodic partners are displayed on the axes. The size of the bubble was scaled with the yield achieved under condition set A (blue) and B (orange). Within the blue area (small differences in oxidation potential) both condition sets achieved similar yields.

Parameter	Unit	Low (–)	High (+)
Current density	mA/cm^2	10	20
Applied charge $F/1$	F	2	3
Ratio phenol:arene	–	1:2.0	1:3.5
Concentration of 1	M	0.2	0.4

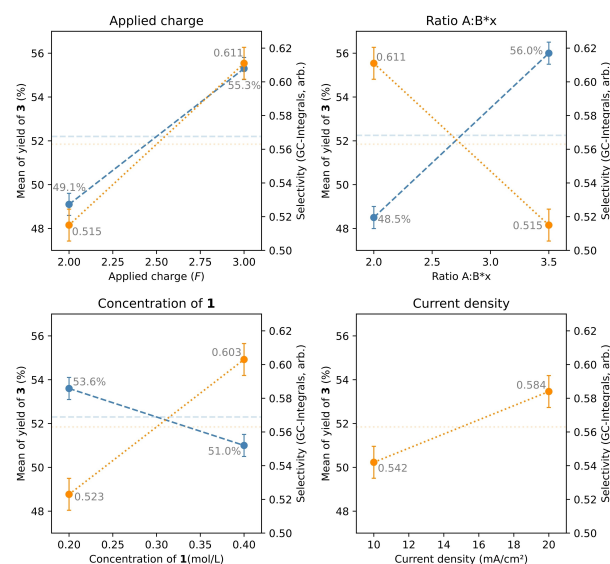


Figure 4. Main effect plots of the initial fractional factorial design of the cross-coupling between 4-methylguaiacol (1) and 2,5-dimethoxytoluene (2). The yield in percent is plotted on the left axis and the ratio of the GC integrals of the minor components to standard normalized to the starting material amount is plotted on the right axis.

the flow, the excess of arene in the investigated range showed the largest main effect (+7% with an increase from 1.0 to 2.5 equivalents). Increasing the applied charge (2.0 *F* to 3.0 *F*) increases the yield by 6%, but the selectivity of the reaction also deteriorates.

Higher concentrations of **1** lower the total yield by 2% and lead to inferior selectivity. The current density had no significant influence on the cross-coupling yield in the investigated range and only a slight negative influence on the selectivity at higher current densities. Therefore, we altered the current density linearly in steps of 5 mA/cm² from 10–85 mA/cm² (Figure 5). The applied charge was lowered to 2.5 *F* with respect to **1**. In the range of 10–40 mA/cm² the yield is above the overall average of the screening, with a maximum at 20 mA/cm². From 45 mA/cm² the yield shows a downward trend to a minimum at the last test point at 85 mA/cm².

The quotient of the GC integral of the remaining phenol with the internal standard shows a minimum at 30 mA/cm² and increases at higher current density, whereas the GC integral of the sum of the GC detectable minor components decreases at higher current density. This can be explained by the simplified oxidative polymerization at the interface. These oligomeric structures can no longer be detected by GC (from tetrameric coupling products and higher masses). We therefore decided to investigate the range between 40 and 80 mA/cm² using DoE, in a 2⁵⁻¹ fractional factorial experimental design (Table 2).

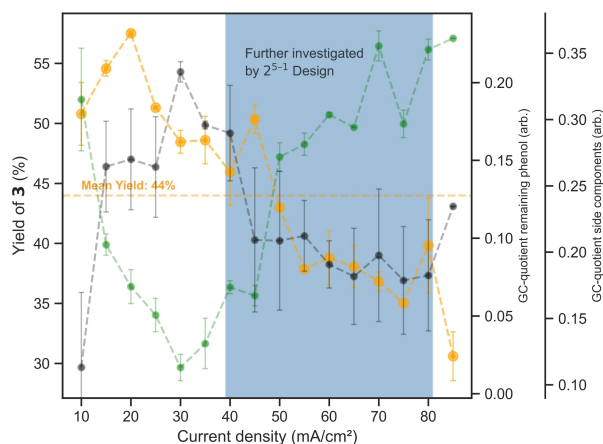


Figure 5. Linear screening of current density of cross-coupling between 4-methylguaiaacol (**1**) and 2,5-dimethoxytoluene (**2**). The yield in % is marked in yellow, the quotient of the GC integrals (FID) of the remaining phenol and the internal standard is marked in green, and the quotient of the sum of the remaining side components and the standard is labelled in black.

Table 2. Parameter settings of the comparing 2 ⁵⁻¹ fractional factorial design.			
Parameter	Unit	Low (–)	High (+)
Current density	mA/cm ²	40	80
Concentration phenol	M	0.1	0.2
Ratio phenol:arene	–	1:2.5	1:3.5
Temperature	°C	25	50
Concentration MTBS	mM	60	120

To increase the selectivity of the electrolysis, further investigation of the applied charge was omitted, and it was left fixed at 2 *F* relative to the phenol used. For this purpose, the temperature was set in the range between room temperature (25 °C) and 50 °C, primarily to investigate the influence of the temperature-induced increase in the diffusion rate. In addition, the amount of supporting electrolyte was included in the optimization to investigate the process stability even at low amounts of supporting electrolyte. A low amount of supporting electrolyte is advantageous for the the electrolysis due to simplified workup as a result of lower reagent waste. Since low amounts of the phenol had a positive effect on yield and selectivity in the first experimental design, the range was shifted to 0.5–1.0 mmol. Each experimental point was performed in duplicate and the central points in triplicate. In addition to the substrate combination **1**+**2** (I), the substrate combination **4**+**5** (III) was also tested under the same conditions and the yield of the cross-coupling reaction as a response was determined. In both cases, the models were backward eliminated with $\alpha=0.05$, and non-significant effects were removed from the models. The models do not show any curvature of the response surface in the investigated area and the fit by multivariate linear regression shows a high goodness of fit of $R^2=81\%$ and 86% , respectively (Figure 6).

As already suspected due to the linear screening, the high current density of 80 mA/cm² achieves a lower yield in both cases than with the lower setting. However, the yield of the cross-coupling reaction with **4** as phenolic component decreases less from 77% to 73% than with **1** from 45% to 35%.

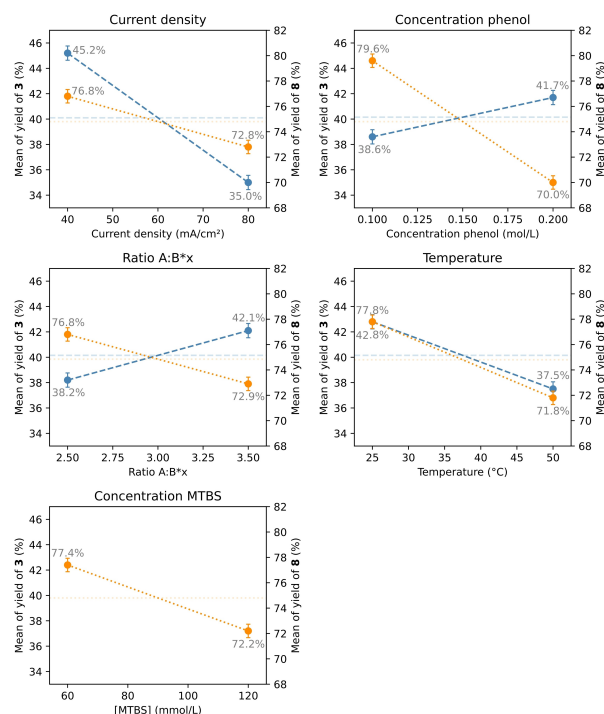


Figure 6. Main effect plots of the second fractional factorial design for the cross-coupling. The yield in percent is plotted for **3** on the left axis and for **8** on the right axis. MTBS = MeNBu₃O₃SOMe.

Elevated temperatures (50 °C) had a similar degrading effect on yield, in both cases by about 5%. Fortunately, the loading of supporting electrolyte had no significant effect in the case of the guaiacol cross-coupling; in the case of the coupling with **4**, the smaller amount of supporting electrolyte showed a yield 5% higher on average than that of the high loading. However, small amounts of supporting electrolyte led to poorer conductivity of the electrolyte and thus to a higher cell voltage in the galvanic electrolysis, especially with a larger inter-electrode gap.

Depending on the phenol in question, cross-coupling with **4** leads to a higher yield with a lower amount of phenol and a lower excess ratio of arene. These conditions improve the atomic economy of the reaction and predict a yield under optimal conditions of 85%. The isolated yield was remarkably close at 79% on the 0.5 mmol scale. In contrast, for the cross-coupling optimized with **1**, a higher starting material amount and a higher arene excess have a positive effect on the yield. To investigate the robustness of the cross-coupling with **4** at even lower surpluses and higher current densities, we experimentally tested it separately in another experimental design. Therefore, the current density (100–150 mA/cm²), the excess of arene (1.0–1.5), and the applied charge (2.0–2.4 F) have been examined in a full factorial 2³ experimental design. The model shows a good linearity of 86% and an average yield of the coupling product of 49%. However, in this investigated range, only the arene excess shows significant influence, with the higher excess increasing the yield from 46% to 53%. Nevertheless, the observation that current density shows no effect in this range is noteworthy; this is consistent with previous studies on cross-coupling of protected phenols in beaker cells.^[30] Based on this result, we investigated the arene equivalents in a linear fashion (step size 0.2 eq.), showing a local maximum of the yield at 2.5 eq., analogous to the finding from the fractional factorial design at lower current densities (Figure 7). The reaction conditions at the local maximum, although 20% lower than those of the fractional design, are only 7% below the original conditions and thus one-thirtieth the electrolysis time required.

We applied the optimized conditions of the fractional factorial models to the substrate combinations (scaling-up by factor of five), but previous experiments had shown that the

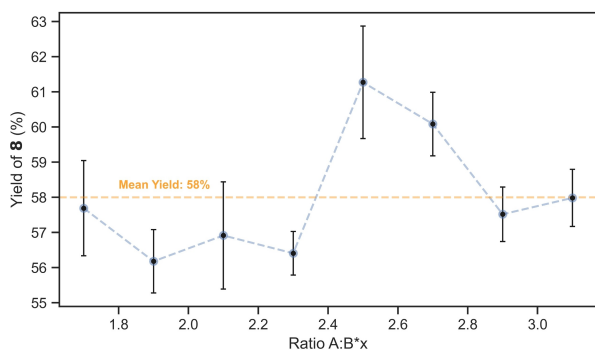


Figure 7. Linear screening of excess equivalents of the arene. Current density $j = 150 \text{ mA/cm}^2$, $Q = 2 F/4$, $T = 25^\circ\text{C}$.

coupling possibility in *ortho*- or *para*-position is the decisive substrate parameter. Therefore, the 2,4-substituted phenols were reacted according to the optimizations of combination I and the coupling reactions employing **4** as phenol according to those of combination III. An increase in the excess ratio, for example in the case of **10**, showed no further increase in yield. Nevertheless, the optimized conditions could be transferred well to other substrates, in the case of the *ortho*-coupling with up to 72% yield in the case of **12**, in the case of the *para* coupling even up to 85% (Figure 8).

Conclusions

By screening in 5 mL Teflon cells, a series of biaryls were successfully synthesized by anodic cross-coupling with BDD electrodes. By evaluating the cyclic voltammetry data of the substrates, it was possible to make an initial grouping of the substrate combinations based on the oxidation potentials. Using the example of the cross-coupling of 4-methylguaiacol (**1**) and 2,5-dimethoxytoluene (**2**), the influence of, among other things, higher current densities up to 20 mA/cm² was first investigated with a partial factorial experimental design, whereby no yield losses occurred at high current densities. A subsequent linear investigation of the current density laid the foundation for a further partial factorial model between 40 and 80 mA/cm². The substrate combination syringol (**4**) and 3,4-dimethoxytoluene (**5**) was also investigated. For the first

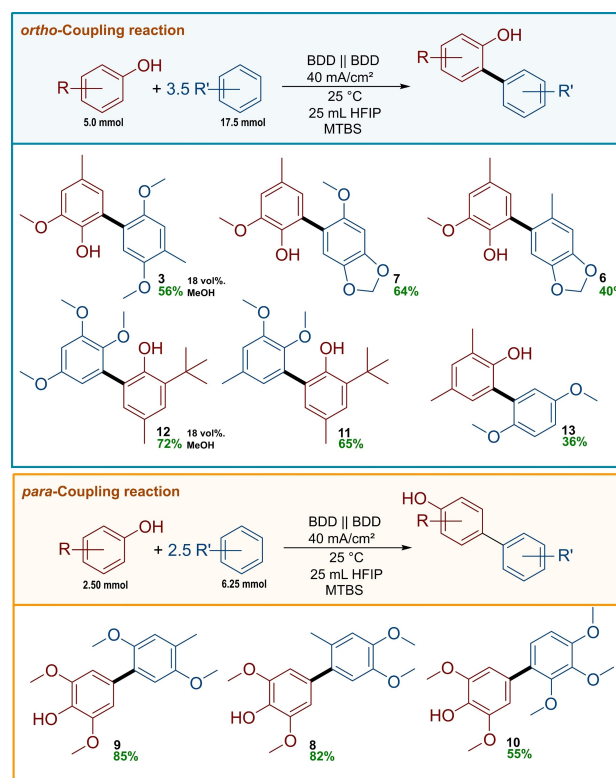


Figure 8. Optimized conditions for the *ortho/para*-cross-coupling and isolated yields. MTBS = MeNBu₃O₃SOME.

combination, electrolysis conditions with a phenol concentration of 0.2 mol/L and a ratio of 1:3.5 proved to be advantageous, while in the second case a lower concentration of 0.1 mol/L but with an advantageously lower ratio of 1:2.5 resulted in higher yields. The parameter space of the second combination was further examined to higher current densities up to 150 mA/cm². An astonishing robustness of this cross-coupling was observed at high current densities with respect to yield and selectivity; the application of 150 mA/cm² still resulted in a yield of 60%. The optimized conditions were successfully transferred to other substrate combinations, with yields of up to 85% isolated in the fivefold scaleup. The different optimized conditions provide a basis for substrate-specific electrolysis conditions, which could be further refined by additional molecular descriptors.

Experimental Section

NMR Spectroscopy

Purified compounds were recorded on a multi-nuclear magnetic resonance spectrometer of the type AV II 400 (Bruker, analytic measuring technique, Karlsruhe, Germany). The chemical shifts were referenced on δ value in ppm of the residual signal of the deuterated solvent (CDCl₃: ¹H = 7.26 ppm, ¹³C = 77.2 ppm).

Gas Chromatography

Reaction mixtures and purified products were analyzed *via* gas chromatography, for which a GC-2010 (Shimadzu, Japan) was used. The column was a quartz capillary column ZB-5 (length: 30 m, inner diameter: 0.025 cm, layer thickness of the stationary phase: 0.25 μ m, carrier gas: hydrogen, stationary phase: (5% phenyl)-methylpolysiloxane, Phenomenex, USA). The detector was a flame ionization detector (FID). The injector temperature was 250 °C with a linear carrier gas rate of 45.5 cm/s. The method "hart" (starting temperature: 50 °C, heating rate: 15 °C/min, end temperature: 290 °C for 8 min) was used for the GC measurements.

Mass Spectrometry

For high-resolution electrospray ionization (ESI) an Agilent 6545 Q-ToF MS was utilized.

Preparative Chromatography

For standard liquid chromatography separation silica gel 60 M (0.040–0.063 mm Macherey-Nagel GmbH & Co., Düren, Germany) was used. An automatic silica flash column chromatography system was used, which consists of a control unit C-620, a fraction collector C-660 and a UV photometer C-635 (Büchi, Flawil, Switzerland). Thin-layer-chromatography was performed using "DC Kieselgel 60 F254" (Merck KGaA, Darmstadt, Germany) on aluminum and a UV lamp (Benda, NU-4 KL, λ = 254 nm, Wiesloch, Germany). The resulting retention factors (R_f) are given in relation to the solvent ratio.

Electrochemical Setup

As DC power source, a HMP4040 device (Rhode&Schwarz, München, Germany) with a controllable DC output of 0–32 V (\pm

1 mV) and 0–10 A (\pm 1 mA) and a maximum power of 160 W per channel was used. All electrolysis reactions were carried out under galvanostatic conditions using a two-electrode set-up. **Cyclic voltammetry** was performed in a 10 mL snap-cap vial equipped with an Autolab PGSTAT101 potentiostat (Metrohm AG, Herisau, Switzerland). WE: BDD tip, 1 mm diameter; CE: glassy carbon rod; RE: Ag/AgCl in saturated LiCl/EtOH. A sweep rate of 100 mV/s was used.

Melting points

Were determined with a Melting Point Apparatus B-565 (Büchi, Flawil, Switzerland) and are uncorrected. Heating rate: 1 °C/min.

Further synthesis information can be found in the supporting information.

Acknowledgements

The authors thank the Deutsche Forschungsgemeinschaft (DFG) in frame of FOR 2982 – UNDODE (Wa1276/24-1) for financial support. M. Hielscher thanks the DFG for founding in the frame of the research training group GRK2516. M. H. thanks Maurice Dörr for proofreading the manuscript. Open Access funding enabled and organized by Projekt DEAL.

Conflict of Interest

The authors declare no conflict of interest.

Keywords: electrochemical cross-coupling · oxidation · design of experiments · reaction optimization · electrolysis

- [1] a) G. Bringmann, A. J. Price Mortimer, P. A. Keller, M. J. Gresser, J. Garner, M. Breuning, *Angew. Chem. Int. Ed.* **2005**, *44*, 5384–5427; *Angew. Chem.* **2005**, *117*, 5518–5563; b) G. Bringmann, T. Gulder, T. A. M. Gulder, M. Breuning, *Chem. Rev.* **2011**, *111*, 563–639; c) K. C. Nicolaou, P. G. Bulger, D. Sarlah, *Angew. Chem. Int. Ed.* **2005**, *44*, 4442–4489; *Angew. Chem.* **2005**, *117*, 4516–4563; d) M. C. Kozłowski, B. J. Morgan, E. C. Linton, *Chem. Soc. Rev.* **2009**, *38*, 3193–320.
- [2] a) R. Noyori, *Angew. Chem. Int. Ed.* **2002**, *41*, 2008–2022; *Angew. Chem.* **2002**, *114*, 2108–2123; b) W. S. Knowles, *Angew. Chem. Int. Ed.* **2002**, *41*, 1998–2007; *Angew. Chem.* **2002**, *114*, 2096–2107; c) W. S. Knowles, *Adv. Synth. Catal.* **2003**, *345*, 3–13; d) A. F. Kiely, J. A. Jernelius, R. R. Schrock, A. H. Hoveyda, *J. Am. Chem. Soc.* **2002**, *124*, 2868–2869; e) J. B. Alexander, D. S. La, D. R. Cefalo, A. H. Hoveyda, R. R. Schrock, *J. Am. Chem. Soc.* **1998**, *120*, 4041–4042; f) H.-U. Blaser (ed.) *Asymmetric catalysis on industrial scale. Challenges, approaches and solutions*, Wiley-VCH, Weinheim, **2004**; g) R. Noyori, *Adv. Synth. Catal.* **2003**, *345*, 15–32.
- [3] a) P. Kirsch, M. Bremer, *Angew. Chem. Int. Ed.* **2000**, *39*, 4216–4235; *Angew. Chem.* **2000**, *112*, 4384–4405; b) A. C. Grimsdale, K. L. Chan, R. E. Martin, P. G. Jokisz, A. B. Holmes, *Chem. Rev.* **2009**, *109*, 897–1091; c) S.-J. Su, D. Tanaka, Y.-J. Li, H. Sasabe, T. Takeda, J. Kido, *Org. Lett.* **2008**, *10*, 941–944; d) P. W. N. M. van Leeuwen, P. C. J. Kamer, C. Claver, O. Pàmies, M. Diéguez, *Chem. Rev.* **2011**, *111*, 2077–2118.
- [4] a) I. Cepanec, *Synthesis of biaryls*, 1. Ed., Elsevier, Amsterdam, **2004**; b) M. Beller, C. Bolm, *Transition Metals for Organic Synthesis. Building blocks and fine chemicals*, 2. Ed., Wiley, Weinheim, **2004**; c) J. Hassan, M. Sévignon, C. Gozzi, E. Schulz, M. Lemaire, *Chem. Rev.* **2002**, *102*, 1359–1470; d) A. de Meijere, F. Diederich, *Metal-Catalyzed Cross-Coupling Reactions*, 2. Ed., Wiley, Weinheim, **2004**; e) A. Zapf, M. Beller, *Top. Catal.* **2002**, *19*, 101–109.

- [5] a) L. Ackermann (ed.) *Modern Arylation Methods*, Wiley, 2009; b) G. Dyker, *Handbook of C–H Transformations. Applications in organic synthesis*, Wiley, Weinheim, Chichester, 2005.
- [6] a) G. A. Molander, N. Ellis, *Acc. Chem. Res.* 2007, 40, 275–286; b) N. Miyaoura, A. Suzuki, *Chem. Rev.* 1995, 95, 2457–2483.
- [7] V. Farina, V. Krishnamurthy, W. J. Scott in *Organic Reactions*, John Wiley & Sons, Inc, Hoboken, NJ, USA, 2004, S. 1–652.
- [8] L. J. Goossen, N. Rodríguez, K. Goossen, *Angew. Chem. Int. Ed.* 2008, 47, 3100–3120; *Angew. Chem.* 2008, 120, 3144–3164.
- [9] E. Negishi, *Acc. Chem. Res.* 1982, 15, 340–348.
- [10] a) C. E. Hartmann, S. P. Nolan, C. S. J. Cazin, *Organometallics* 2009, 28, 2915–2919; b) P. Knochel, *Handbook of Functionalized Organometallics. Applications in synthesis*, Wiley, Weinheim, Chichester, 2005; c) T. J. Korn, M. A. Schade, S. Wirth, P. Knochel, *Org. Lett.* 2006, 8, 725–728; d) R. Martin, S. L. Buchwald, *J. Am. Chem. Soc.* 2007, 129, 3844–3845; e) I. Sapountzis, W. Lin, C. C. Kofink, C. Despotopoulou, P. Knochel, *Angew. Chem. Int. Ed.* 2005, 44, 1654–1658; *Angew. Chem.* 2005, 117, 1682–1685; f) K. Tamao, K. Sumitani, M. Kumada, *J. Am. Chem. Soc.* 1972, 94, 4374–4376.
- [11] a) D. Alberico, M. E. Scott, M. Lautens, *Chem. Rev.* 2007, 107, 174–238; b) T. A. Dwight, N. R. Rue, D. Charyk, R. Josselyn, B. De Boef, *Org. Lett.* 2007, 9, 3137–3139; c) A. Jean, J. Cantat, D. Bérard, D. Bouchu, S. Canesi, *Org. Lett.* 2007, 9, 2553–2556; d) D. R. Stuart, K. Fagnou, *Science* 2007, 316, 1172–1175.
- [12] a) T. Dohi, M. Ito, K. Morimoto, M. Iwata, Y. Kita, *Angew. Chem. Int. Ed.* 2008, 47, 1301–1304; *Angew. Chem.* 2008, 120, 1321–1324; b) M. Grzybowski, K. Skonieczny, H. Butenschön, D. T. Gryko, *Angew. Chem. Int. Ed.* 2013, 52, 9900–9930; *Angew. Chem.* 2013, 125, 10084–10115; c) I. Hussain, T. Singh, *Adv. Synth. Catal.* 2014, 356, 1661–1696; d) N. Y. More, M. Jeganmohan, *Eur. J. Org. Chem.* 2017, 2017, 4305–4312; e) K. Morimoto, K. Sakamoto, Y. Ohnishi, T. Miyamoto, M. Ito, T. Dohi, Y. Kita, *Chem. Eur. J.* 2013, 19, 8726–8731; f) C. A. Mulrooney, X. Li, E. S. DiVirgilio, M. C. Kozlowski, *J. Am. Chem. Soc.* 2003, 125, 6856–6857; g) T. Quell, N. Beiser, K. M. Dyballa, R. Franke, S. R. Waldvogel, *Eur. J. Org. Chem.* 2016, 2016, 4307–4310; h) T. Quell, M. Mirion, D. Schollmeyer, K. M. Dyballa, R. Franke, S. R. Waldvogel, *ChemistryOpen* 2015, 5, 115–119; i) A. A. O. Sarhan, C. Bolm, *Chem. Soc. Rev.* 2009, 38, 2730–2744; j) S. R. Waldvogel, S. Trosien, *Chem. Commun.* 2012, 48, 9109–9119; k) S. B. Beil, T. Müller, S. B. Sillart, P. Franzmann, A. Bomm, M. Holtkamp, U. Karst, W. Schade, S. R. Waldvogel, *Angew. Chem. Int. Ed.* 2018, 57, 2450–2454; *Angew. Chem.* 2018, 130, 2475–2479; l) M. Schubert, S. R. Waldvogel, *Eur. J. Org. Chem.* 2016, 2016, 1921–1936.
- [13] A. Libman, H. Shalit, Y. Vainer, S. Narute, S. Kozuch, D. Pappo, *J. Am. Chem. Soc.* 2015, 137, 11453–11460.
- [14] a) J. L. Röckl, D. Pollok, R. Franke, S. R. Waldvogel, *Acc. Chem. Res.* 2020, 53, 45–61; b) S. R. Waldvogel, S. Lips, M. Selt, B. Riehl, C. J. Kampf, *Chem. Rev.* 2018, 118, 6706–6765; c) A. Wiebe, T. Gieshoff, S. Möhle, E. Rodrigo, M. Zirbes, S. R. Waldvogel, *Angew. Chem. Int. Ed.* 2018, 57, 5594–5619; *Angew. Chem.* 2018, 130, 5694–5721; d) D. Pollok, S. R. Waldvogel, *Chem. Sci.* 2020, 11, 12386–12400; e) J. L. Röckl, D. Schollmeyer, R. Franke, S. R. Waldvogel, *Angew. Chem.* 2020, 132, 323–327; f) K. D. Moeller, *Chem. Rev.* 2018, 118, 48107–4833; g) E. J. Horn, B. R. Rosen, P. S. Baran, *ACS Cent. Sci.* 2016, 2, 302–308; h) R. Daniel Little, K. D. Moeller, *Electrochem. Soc. Interface* 2002, 11, 36–42; i) R. Francke, R. D. Little, *Chem. Soc. Rev.* 2014, 43, 2492–2521.
- [15] a) G. Hilt, K. I. Smolko, *Angew. Chem. Int. Ed.* 2001, 40, 3399–3402; *Angew. Chem.* 2001, 113, 3514–3516; b) Y. Yuan, A. Lei, *Nat. Commun.* 2020, 11, 802; c) B. A. Frontana-Urbe, R. D. Little, J. G. Ibanez, A. Palma, R. Vasquez-Medrano, *Green Chem.* 2010, 12, 2099.
- [16] J. Seidler, J. Strugatchi, T. Gärtner, S. R. Waldvogel, *MRS Energy Sustainability* 2020, 7, E42.
- [17] a) G. H. M. de Kruijff, T. Goschler, L. Derwich, N. Beiser, O. M. Türk, S. R. Waldvogel, *ACS Sustainable Chem. Eng.* 2019, 7, 10855–10864; b) M. Selt, B. Gleede, R. Franke, A. Stenglein, S. R. Waldvogel, *J. Flow Chem.* 2021, 11, 143–162.
- [18] S. B. Beil, D. Pollok, S. R. Waldvogel, *Angew. Chem. Int. Ed.* 2021, 60, 14750–14759; *Angew. Chem.* 2021, 133, 14874–14883.
- [19] a) T. Gieshoff, D. Schollmeyer, S. R. Waldvogel, *Angew. Chem. Int. Ed.* 2016, 55, 9437–9440; *Angew. Chem.* 2016, 128, 9587–9590; b) O. Hollóczki, R. Macchieraldo, B. Gleede, S. R. Waldvogel, B. Kirchner, *J. Phys. Chem. Lett.* 2019, 10, 1192–1197; c) Y. Imada, J. L. Röckl, A. Wiebe, T. Gieshoff, D. Schollmeyer, K. Chiba, R. Franke, S. R. Waldvogel, *Angew. Chem. Int. Ed.* 2018, 57, 12136–12140; *Angew. Chem.* 2018, 130, 12312–12317; d) L. Schulz, S. Waldvogel, *Synlett* 2019, 30, 275–286; e) A. Wiebe, D. Schollmeyer, K. M. Dyballa, R. Franke, S. R. Waldvogel, *Angew. Chem. Int. Ed.* 2016, 55, 11801–11805; *Angew. Chem.* 2016, 128, 11979–11983.
- [20] L. Schulz, M. Enders, B. Elsler, D. Schollmeyer, K. M. Dyballa, R. Franke, S. R. Waldvogel, *Angew. Chem. Int. Ed.* 2017, 56, 4877–4881; *Angew. Chem.* 2017, 129, 4955–4959.
- [21] A. Wiebe, S. Lips, D. Schollmeyer, R. Franke, S. R. Waldvogel, *Angew. Chem. Int. Ed.* 2017, 56, 14727–14731; *Angew. Chem.* 2017, 129, 14920–14925.
- [22] a) S. Lips, S. R. Waldvogel, *ChemElectroChem* 2019, 6, 1649–1660; b) S. R. Waldvogel, A. Kirste, S. Mentizi in *Topics in current chemistry*, Vol. 320 (ed.: M. Heinrich, A. Gansäuer), Springer Berlin Heidelberg, Berlin, Heidelberg, 2012, S. 1–31; c) N. Yang, S. Yu, J. V. Macpherson, Y. Einaga, H. Zhao, G. Zhao, G. M. Swain, X. Jiang, *Chem. Soc. Rev.* 2019, 48, 157–204.
- [23] a) I. M. Malkowsky, C. E. Rommel, K. Wedeking, R. Fröhlich, K. Bergander, M. Nieger, C. Quaiser, U. Griesbach, H. Pütter, S. R. Waldvogel, *Eur. J. Org. Chem.* 2006, 2006, 241–245; b) A. Kirste, M. Nieger, I. M. Malkowsky, F. Stecker, A. Fischer, S. R. Waldvogel, *Chem. Eur. J.* 2009, 15, 2273–2277; c) J. Barjau, P. Königs, O. Kataeva, S. Waldvogel, *Synlett* 2008, 5, 2309–2312.
- [24] a) M. Dörr, J. L. Röckl, J. Rein, D. Schollmeyer, S. R. Waldvogel, *Chem. Eur. J.* 2020, 26, 10195–10198; b) M. M. Hielscher, B. Gleede, S. R. Waldvogel, *Electrochim. Acta* 2021, 368, 137420; c) M. Dörr, M. M. Hielscher, J. Proppe, S. R. Waldvogel, *ChemElectroChem* 2021, 8, 2621–2629.
- [25] A. G. Maldonado, G. Rothenberg, *Chem. Soc. Rev.* 2010, 39, 1891–1902.
- [26] A. Kirste, B. Elsler, G. Schnakenburg, S. R. Waldvogel, *J. Am. Chem. Soc.* 2012, 134, 3571–3576.
- [27] A. Kirste, G. Schnakenburg, F. Stecker, A. Fischer, S. R. Waldvogel, *Angew. Chem. Int. Ed.* 2010, 49, 971–975; *Angew. Chem.* 2010, 122, 983–987.
- [28] S. Lips, A. Wiebe, B. Elsler, D. Schollmeyer, K. M. Dyballa, R. Franke, S. R. Waldvogel, *Angew. Chem. Int. Ed.* 2016, 55, 10872–10876; *Angew. Chem.* 2016, 128, 11031–11035.
- [29] a) B. Dahms, R. Franke, S. R. Waldvogel, *ChemElectroChem* 2018, 5, 1249–1252; b) B. Riehl, K. Dyballa, R. Franke, S. Waldvogel, *Synthesis* 2016, 49, 252–259.
- [30] A. Wiebe, B. Riehl, S. Lips, R. Franke, S. R. Waldvogel, *Sci. Adv.* 2017, 3, eaao3920.
- [31] L. Schulz, R. Franke, S. R. Waldvogel, *ChemElectroChem* 2018, 5, 2069–2072.
- [32] a) S. Lips, B. A. Frontana-Urbe, M. Dörr, D. Schollmeyer, R. Franke, S. R. Waldvogel, *Chem. Eur. J.* 2018, 24, 6057–6061; b) S. Lips, D. Schollmeyer, R. Franke, S. R. Waldvogel, *Angew. Chem. Int. Ed.* 2018, 57, 13325–13329; *Angew. Chem.* 2018, 130, 13509–13513.

Manuscript received: September 13, 2021
Revised manuscript received: September 27, 2021
Accepted manuscript online: September 27, 2021